

## AN IMPROVED DISCRETE ELEMENT METHOD FOR STABILITY ANALYSIS OF TUNNELS IN ROCK MASS\*

N. HATAF\*\* AND M. BAHARLOO

Dept. of Civil Engineering, Shiraz University, Shiraz, I. R. of Iran  
Email: hataf@shirazu.ac.ir

**Abstract** – Rock masses supporting a tunnel often have natural cracks and joints which must be detected and analyzed at excavation to assess tunnel stability. Mathematically, these are discontinuities that must be embedded in the finite element model of the excavation to improve reliability. Because direct consideration of cracks as mathematical discontinuities in excavation models presents considerable computational and analytical challenge, a simple discrete element model (DEM) has been used to analyze the stability of tunnels in jointed rocks. This model, which is a member of the DEM group, has the advantage of being able to model large displacements and behavior of highly fractured rock masses. The low volume of numerical computing and high speed in analysis are other advantages of the used model.

A new algorithm for detecting contact points between blocks has been used to improve the model. Different examples and case studies have been solved successfully using this modified discrete element model.

**Keywords** – Rock, joints, discrete element, contact points, tunnel, stability

### 1. INTRODUCTION

Analysis of rock mass behavior without considering the effect of existing discontinuities would not give a good image of the actual behavior of the rock mass in many cases. In other words, the presence of cracks and discontinuities has an essential role in the behavior of rock mass under applied forces. The physical behavior of such a system is the opening of discontinuities and sliding along them. Therefore deformation of the system is governed by the sliding of blocks on each other. Although the behavior of intact rock is elastic, the presence of these discontinuities may lead to the nonlinear behavior of the rock mass. The existing continuum models are not able to simulate the discontinuous masses such as highly jointed rocks, properly. Thus the need for a tool to model the effect of these discontinuities, for the rock masses with cracks and joints is quite obvious. Researchers have attempted to develop discontinuum models such as finite, joint and distinct element approaches since 1968. In this paper, having reviewed the various discontinuum models, the use of a simple model to consider the effect of discontinuities is presented.

Goodman *et al.* [1] used a finite element method along with joint elements to model the behavior of rock blocks. The joints were assumed rectangles with zero widths and four nodes each on their corners. Having considered two degrees of freedom for each node, the number of degrees of freedom for the element is eight. Ghaboussi *et al.* [2] modified the joint element by reducing the number of degrees of freedom and therefore reducing the volume of computation. According to this model, the relative displacements of the surface of the elements are considered as independent degrees of freedom, thus the degrees of freedom on sliding surfaces changes to the relative displacement of two sliding surfaces. Zienkiewicz *et al.* [3] and Burman [4] also used finite and joint element methods. Zienkiewicz *et al.* analyzed the rock masses as no tension materials and Burman considered the intact rocks as rigid elements and the contacts between the adjacent blocks as joint elements.

\*Received by the editors November 20, 2001 and in final revised form January 13, 2003

\*\*Corresponding author

Although these early developments succeeded in simulating discontinuities, they could not easily handle rock masses with large joints and crack densities. These situations increase the number of degrees of freedom, the size of stiffness matrix and when large displacements occur, rearrangement of finite element mesh is required, which is a very difficult task.

Cundall [5] simulated rock masses by assuming them as blocks that are in contact with each other in edge-to-edge and corner to edge arrangements. Normal and shear springs were assumed at contact points. Forces were generated in the springs at the contact points due to the relative displacement of these nodes. The governing force-displacement equations along with the equations of motion of elements were solved simultaneously to simulate large displacements. This method is therefore one of the most proper ones in analyzing the discontinuous masses. It suffers, however, some shortcomings such as its sensitivity to the values of damping ratios. On the other hand, since the block relaxation takes place one by one the simulation is path dependent.

Kawai [6] proposed another discontinuous model in which the elements were assumed rigid and their contact was through a set of springs spreading on their common surfaces. Due to the type of contact assumed between the blocks, this method was not able to simulate large displacements easily.

Belytschko *et al.* [7] introduced a static simple model similar to Kawai's model. In this model, a point was defined on the contact surface of two adjacent elements as "slave point". The contact surface between elements was fixed and only change in contact area and/or element penetration was possible. Since the change in contact area and the amount of penetration of blocks were restricted, simulation of large displacement was difficult in this method.

Following Cundall [5], Stewart and Brown [8] proposed a similar block relaxation simulation, but the elements were relaxed one by one and static equilibrium equations were used to calculate the displacements. In this model, the problem of damping factor effect was removed, but the path dependency problem still existed.

Despite these shortcomings, the concept of block elements was later applied for stability analysis of soil slopes by Ching [9]. Wang and Garga [10, 11] proposed a new model called block-spring model, in which the static equilibrium equations and force displacement relations were used to obtain the contact forces. This model was able to simulate large displacement, but it did not have the problem of damping factor effect and path dependency as observed in the previously cited methods.

In this paper, the principles of Wang and Garga's block-spring model [10], for its simplicity and its capability to simulate large displacements, is used to analyze the behavior of rock masses. A special algorithm is developed to improve the abilities and accuracy of the method and a number of examples are solved. Wang and Garga [10] explained the theory of the Block-spring model in details and the main points are only presented here.

## 2. METHODS

In order to better understand the Wang and Garga [10] model, we refer to the left hand side of Fig.1 which shows the edge-to-edge and to the right hand side of the figure that displays the corner-to-edge contact. Two springs are assumed at each contact point (normal and shear). The relative displacements of the contact points lead in generating normal and shear forces in the springs. By simultaneous solution of static equilibrium equations and force-displacement equations for these springs at contact points, the forces and displacement of these points are calculated. The contact forces are calculated incrementally and the values obtained at each step are accumulated as follows:

$$F_n^{new} = F_n^{old} + \Delta F_n, \quad F_s^{new} = F_s^{old} + \Delta F_s \quad (1)$$

In which  $F_n$  and  $F_s$  are normal and shear forces at contact point respectively, and

$$\Delta F_n = K_n' \Delta_n, \quad \Delta F_s = K_s' \Delta_s \quad (2)$$

In Eq. (2)  $\Delta_n$  and  $\Delta_s$  are normal and shear displacements of the springs and  $K'_n$  and  $K'_s$  are normal and shear stiffnesses of the springs in force per unit length. The above equations along with the static equilibrium equations (i.e.  $\sum F = 0$  in which  $\sum F$  is the sum of all forces applied on the element including contact, gravity and external forces) are solved to calculate the contact forces and displacement values.

**a) Spring stiffness**

To calculate the spring stiffnesses, the model proposed by Hamajima and Kawai [12] is used. In this model, the normal and shear stiffness of the springs are given as follows

$$k_s = \frac{E}{1 + \nu} \tag{3}$$

$$k_n = \frac{E}{1 - \nu^2} \tag{4}$$

in force per square length. In Eqs. (3) and (4),  $E$  is modulus of elasticity and  $\nu$  is Poisson's ratio of rock.

For a discontinuum environment, or in other words for rock masses with high density of cracks and joints referring to Fig. 2, it is assumed that a weakness surface called zero element with zero width exists between elements 1 and 2. The shear stiffness of elements 1 and 2 are  $K_{s1}$  and  $K_{s2}$ , which could be determined using Eq. (3). The stiffness of discontinuous surface,  $K_{s0}$ , is determined using the results of the direct shear test.

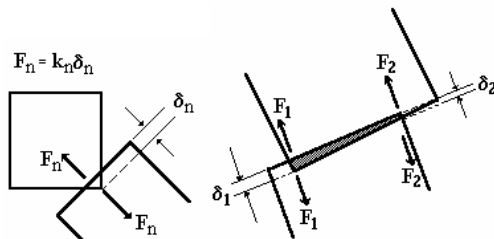


Fig. 1. Contact type in distinct element method

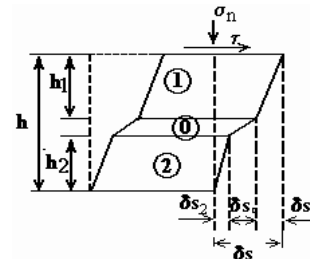


Fig. 2. Discontinuous element [14]

In equilibrium condition, the stress-strain relation of the cited elements is

$$d\tau = k_{s1} \frac{d\delta_{s1}}{h_1} = k_{s2} \frac{d\delta_{s2}}{h_2} = k_{s0} d\delta_{s0} = k_s d\delta_s \tag{5}$$

In which  $h_1$  and  $h_2$  are the distances between the discontinuity surface to gravity center of elements 1 and 2;  $d\delta_{s1}$  and  $d\delta_{s2}$  are shear displacements of elements 1 and 2,  $d\delta_{s0}$  is shear displacement of discontinuity element.  $K_s$  is shear stiffness between gravity centers of elements 1 and 2 and  $\tau$  is shear stress. Since  $d\delta_s = d\delta_{s1} + d\delta_{s2} + d\delta_{s0}$ , the following relation for the equivalent shear stiffness could be obtained

$$k_s = \frac{1}{h_1/k_{s1} + h_2/k_{s2} + 1/k_{s0}} \tag{6}$$

With a similar method the equivalent normal stiffness could be determined

$$k_n = \frac{1}{h_1/k_{n1} + h_2/k_{n2} + 1/k_{n0}} \tag{7}$$

In which  $k_{n1}$  and  $k_{n2}$  are normal stiffnesses of elements 1 and 2 that can be obtained from Eq. (4).  $K_{n0}$  is stiffness of the discontinuous surface and other parameters which were described earlier. It should be mentioned that equivalent normal stiffness might also be obtained using an unconfined compression test on cracked specimen of rock.

### b) Rock bolt simulation

A simple model is applied to simulate the rock bolt effect. The rock bolt is assumed to be anchored at both ends and the side friction is ignored. The rock bolt is replaced by a spring having an axial stiffness,  $K_b$  (Fig. 3). A rigid-plastic criteria is used to simulate the failure at both ends and an elasto-plastic criteria is used for simulating the yielding of the rock bolt material.

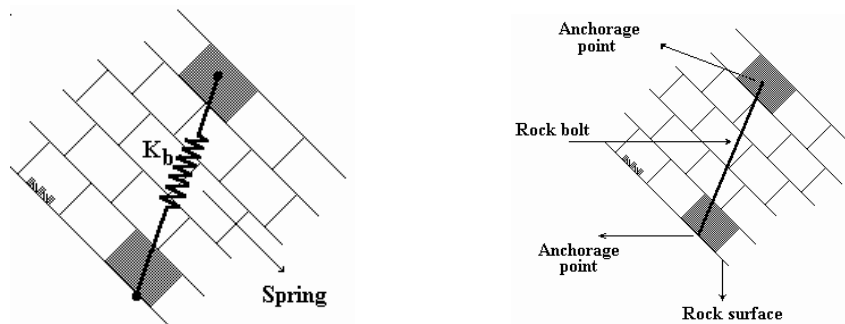


Fig. 3. The equivalent spring model for rock bolt

### c) Ground water pressure effect

The effect of ground water in reducing normal pressure on the surface of discontinuities is considered. The effects of water pressure within rock blocks are ignored.

## 3. MODIFICATIONS MADE TO BLOCK-SPRING MODEL

To simulate the behavior of rock masses with joints and cracks we should use methods that are able to accommodate large displacements. Since such displacements lead to change in element arrangements and thus a change in contact points, we need a proper algorithm to detect these changes and define the new contact points. An algorithm which was developed and used for this purpose is described as follows:

### a) Determination of contact points

To determine the contact points that are continuously changing, a proper algorithm is needed. The stiffness matrices should also be determined at different steps of calculations. Tran and Nelson [13] proposed a new algorithm for granular environment. We modified and used this algorithm for determination of contact points between blocks. The major modification to the algorithm was applying the effective contact length in calculating the equivalent stiffness of springs. The effects of these modifications in increasing the accuracy of deformation values and decrease in computation time are considerable and satisfactory as will be illustrated later in this paper.

### b) Determination of effective contact length

By contact of elements we mean the element penetration. This assumption causes the springs to activate and therefore the development of contact forces. Of course the value of elements' penetration is so small that this assumption makes no considerable error. We consider two types of contacts. The first is simple contact in which contacts between adjacent elements are in two points, (Fig. 4). The second is complex contact in which the number of contact points is more than two (Fig. 5). This type of contact is more suitable for granular materials. To determine the contact points of the elements (i.e., the points of contact of faces) the

equations of the lines of faces are used. To reduce the computation time however, the number of lines to be examined for determination of contact points should be reduced. For this purpose a box around each element is determined as shown in Fig. 6 and the lines that are located in this box are found. The examination of contact points of adjacent elements is then only limited to the lines located in the overlapping regions of adjacent boxes related to each element. This is shown as the shaded area in Fig. 7.

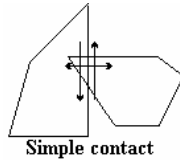


Fig. 4. Simple contact

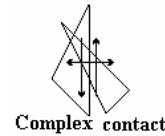


Fig. 5. Complex contact

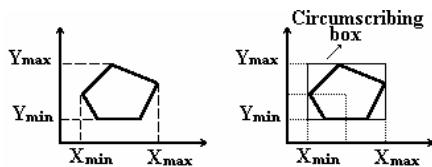


Fig. 6. The datum and the surrounding box

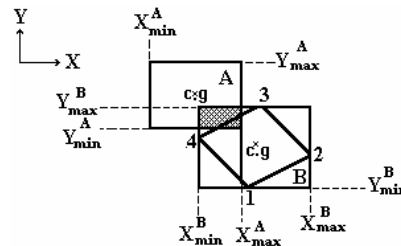


Fig. 7. The overlapping regions of the boxes

Then the intersection points located in the overlapping regions are only considered and other points such as point "I" which is not in overlapping region, is ignored (Fig. 8). Having determined the contact points, the effective contact length,  $L_e$ , is then calculated as follows:

$$L_e = \sqrt{(X_{p1}^2 - X_{p2}^2) + (Y_{p1}^2 - Y_{p2}^2)} \quad (8)$$

where  $X_{p1}, X_{p2}, Y_{p1}$  and  $Y_{p2}$  are the coordinates of the contact points (Fig. 9). While the analysis is in progress, the effective length and the corresponding stiffness are recalculated repeatedly.

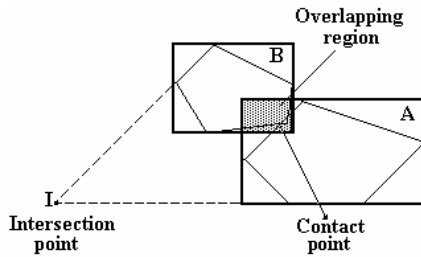


Fig. 8. The contact and intersection points

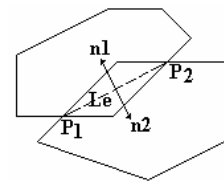


Fig. 9. The effective contact length

**c) Block diagram of the model**

Using the cited modified block-spring model, a computer code (DETUN) has been developed which is able to analyze the behavior of tunnels in jointed rocks. Baharloo [14] presented the program in detail. The code flow chart is illustrated in Fig. 10.

**4. RESULTS AND DISCUSSION**

The program described has been run to solve a number of classic problems for validation of the model and to illustrate its advantages to the previous methods [14] that have not presented here for the sake of brevity. The following examples have been analyzed and compared with the published results to show the typical abilities of the model. It is, thereafter shown that the computer code DETUN could be implemented in analysis of stability of tunnels in jointed rock successfully.

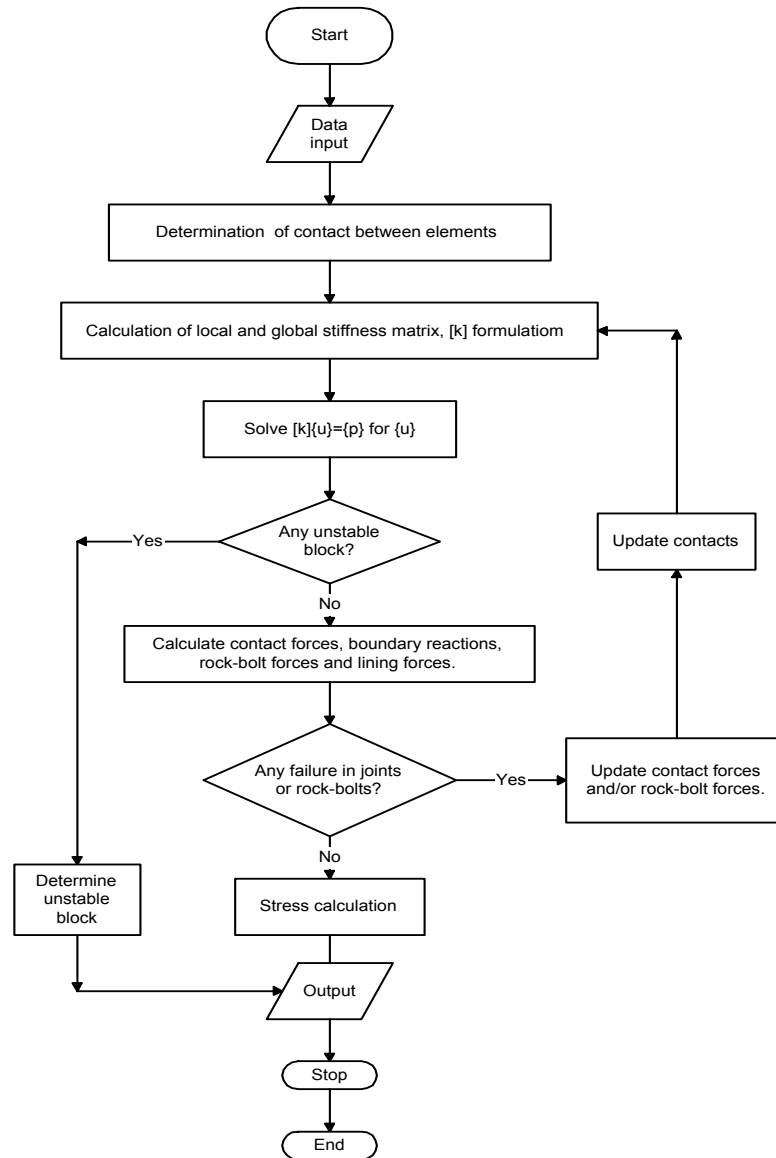


Fig. 10. Flow chart of computer code DETUN

**Example 1: Simulation of large displacement:** Fig. 11 shows the slide of a block on a slope surface analyzed by DETUN to show the capability of the program to simulate large displacements. In this example, the shear strength between blocks 1 and 3 has been chosen to be less than the shear stress developed between these two blocks, resulting in sliding of block 3. During the process of sliding, the new contact points are developed and the small displacement of each step sums to previous displacements.

At each step, the contact points between all blocks are determined by the algorithm described earlier. When block 3 reaches block 2 the stiffness matrix is revised for the new contact points and the equilibrium condition is satisfied, therefore the system becomes stable.

**Example 2: Stability analysis of an underground tunnel:** In this example, the boundary conditions and the applied forces shown in Figs. 12 and 13 are borrowed from Rodrigues Prez geometry [11]. The characteristics of the materials are presented in Table 1. These authors used the finite element method developed by Goodman *et al.* [1] to evaluate the stability of a five stage excavated underground tunnel. The first stage is most critical with respect to other stages. The equivalent stress of 69 kPa was used to approximately simulate the rock bolt effect. The stability analysis of the tunnel for the first stage has therefore been performed by DETUN [14].

As shown in Fig. 14, four sections around the tunnel have been considered. The values of displacements for these sections have been calculated by different methods for comparison.

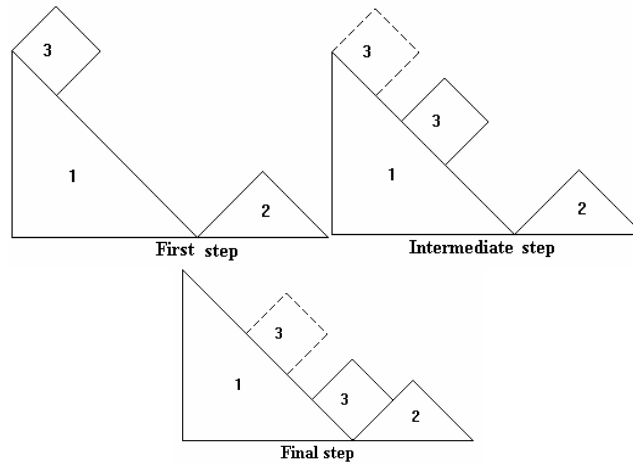


Fig. 11. Analysis of sliding of a block on a slope surface

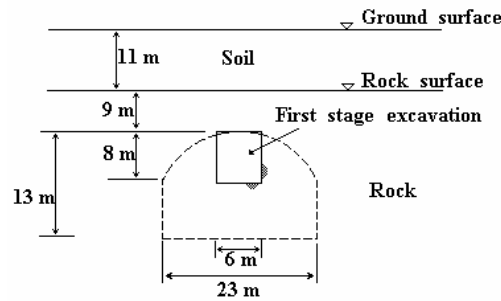


Fig. 12. Section of excavated tunnel, example 2 [11]

Table 1. Properties of materials, example 2 ( $P_i=69$  KPa)

Property	Joint	Shear zone	Intact rock
Young's modulus E (MPa)	—	3.45e3	6.89e3
Poisson's ratio	—	0.30	0.15
Cohesion (MPa)	0	0	34.5
Friction angle (Deg.)	15	35	45
Shear stiffness $K_s$ (KN/m <sup>3</sup> )	1.36e5	—	—
Unit weight (KN/m <sup>3</sup> )	—	25.93	25.93

Foliated metamorphic rock, Jointed rock with shear zone.  
 Rock : Unweathered to slightly weathered schist & gneiss  
 Joints: smooth, planar, usually tight but occasionally open, weathered near the surface.

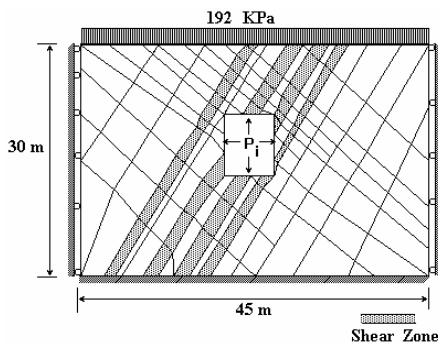


Fig. 13. Discontinuity and boundary conditions

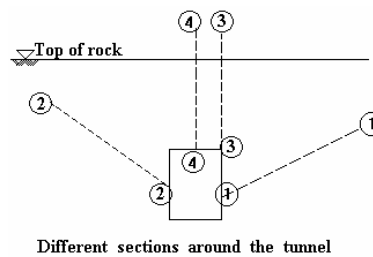


Fig. 14. Sections around the tunnel

Figures 15 to 18 show the results of these comparisons. In these figures the results of FEM, the original block-spring model (Wang & Garga, “Blosmer”) and the DETUN calculations are presented, along with the actual values measured in the field. It can be seen that the modified block-spring model used in DETUN in most cases resulted in a better prediction of displacement compared to the original model. This is due to the algorithm used in the program to determine the contact points, and thus, the more accurate stiffness matrices obtained in each step of computation. Note that all the displacements are along the directions of the cross sections chosen.

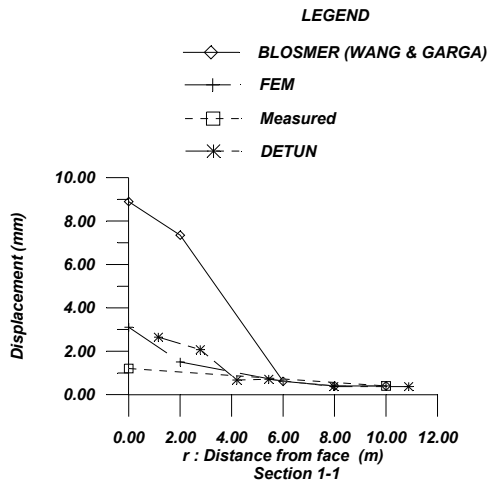


Fig. 15. Comparison of results (section 1-1)

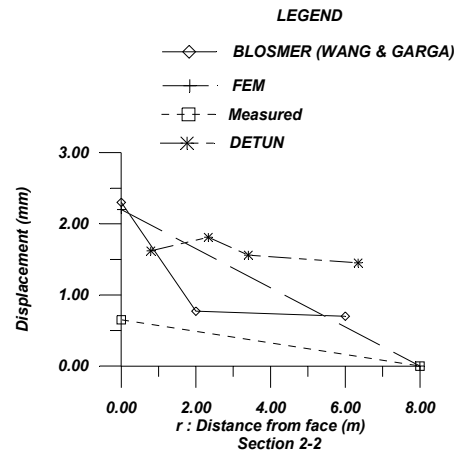


Fig. 16. Comparison of results (section 2-2)

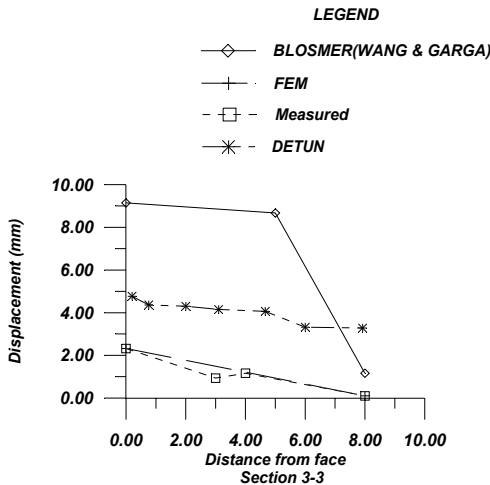


Fig. 17. Comparison of results (section 3-3)

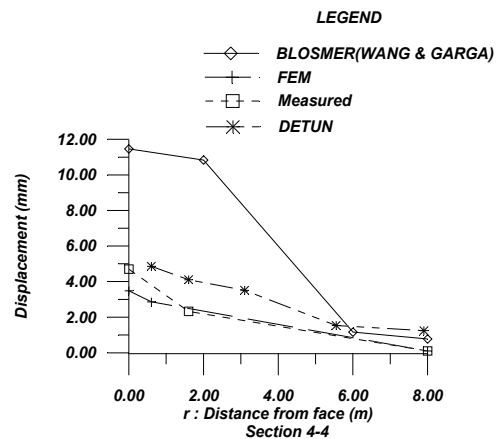


Fig. 18. Comparison of results (section 4-4)

**Example 3: Two adjacent tunnels:** In Fig. 19 the mesh around two adjacent tunnels "a" and "b" is presented. The geometry and the boundary condition of the problem are also presented in the figure. Gravity forces are only considered in this case. In the rock mass around the tunnel, a discontinuous surface (D) and a set of joints are considered. The properties of the rock mass and discontinuities are illustrated in Table 2. In order to investigate the effect of the discontinuities on the behavior of the tunnels, two cases are considered: one with the discontinuity surface D, and the other without it. Figure 20 shows the principal stress distribution for these two cases. It can be seen that in case 1, because of the effect of surface D that transfers the stresses less than the intact rock, the stresses resulting from excavation of tunnel "a" are concentrated on one side and mainly around "a". In case two however, in which the discontinuity D is eliminated, the stress concentration is much less than in case one due to the proper transfer of stresses.



**Example 4: Ground water effect on a tunnel adjacent to a slope:** The stability of a tunnel close to a slope is illustrated in this example. Figure 21 shows the geometry, boundary conditions and the surcharge (520 KPa) of the slope in which a tunnel is excavated. The rock mass is considered to have two sets of joints approximately perpendicular to each other. The properties of the discontinuities and the rock mass are given in Table 3. The stability analysis has been carried out for two cases again; firstly the slope is considered to be completely dry and secondly the water table has been considered as in Fig. 21. In the later case, it is assumed that the speed of tunnel excavation is such that the water table is stable as shown.

For the tunnel to be stable and the blocks not to slide into the tunnel an equivalent uniform rock bolt pressure of 80 KPa was applied to the tunnel. The cases have been analyzed by DETUN. For two arbitrary sections 1-1 and 2-2, as shown in Fig. 22, the values of the displacement for two cases, dry (low water table) and saturated (high water table), have been presented for comparison, in Fig. 23 and 24. As it can be seen the displacements in saturated case are more than those in dry condition, which is due to the effect of pore pressure in reducing the normal stresses and therefore shear strength of the rock mass along with the discontinuities. However, in this special case the ground water effect is not considerable.

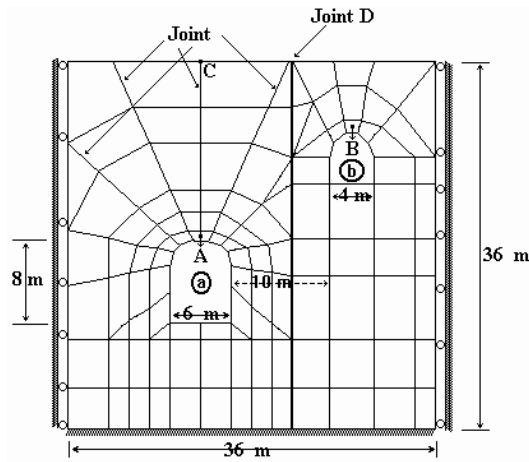


Fig. 19. The condition of two adjacent tunnels, example 3

Table 2. Properties of the rock and discontinuities, example 3

property	Intact rock	Joint
Young's modulus (KPa)	4e7	—
Poisson's ratio	0.25	—
Cohesion (KPa)	200	100
Friction angle(Deg )	35	20
Unit weight (KN/m <sup>3</sup> )	26.0	—
Shear stiffness K <sub>s</sub> (KN/m <sup>3</sup> )	—	1e5
Normal stiffness K <sub>n</sub> (KN/m <sup>3</sup> )	—	1e6
K <sub>0</sub>	0.0	—
case 1: Tunnel <u>a</u> and <u>b</u> with joint <u>D</u> , case 2: Tunnel <u>a</u> and <u>b</u> without joint <u>D</u>		

Table 3. Properties of material in example 4 (P<sub>i</sub>=80 KPa)

property	Joint set 1	Joint set 2	Intact rock
Young's modulus E (KPa)	—	—	4e7
Poisson's ratio	—	—	0.25
Cohesion (KPa)	0	0	200
Friction angle (Deg.)	25	20	35
Shear stiffness K <sub>s</sub> (KN/m <sup>3</sup> )	1e5	2.6e4	—
Unit weight (KN/m <sup>3</sup> )	—	—	25.93

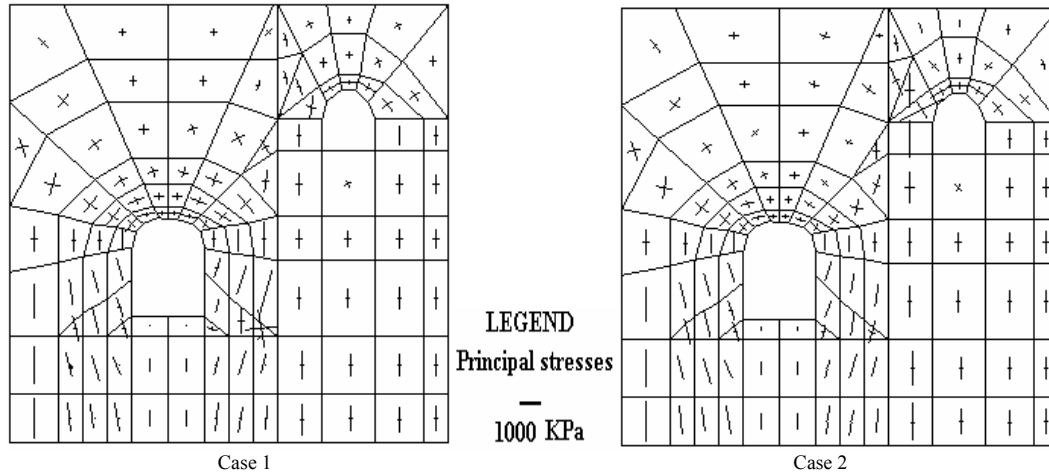


Fig. 20. Principal stresses, example 3

**Effect of incremental loading:** The effect of incremental loading (i.e. loading by steps) on the values of displacements is considered in dry condition of example 4 (Figs. 25 and 26). As it can be seen, when the loading (i.e. 520 KPa) is exerted in one, two and eight steps, the displacements for sections 1-1 and 2-2 decrease. This decrease, however is almost stopped when the loading increment is increased to more than eight steps. The accuracy in displacement calculation therefore is increased when loading is done incrementally.

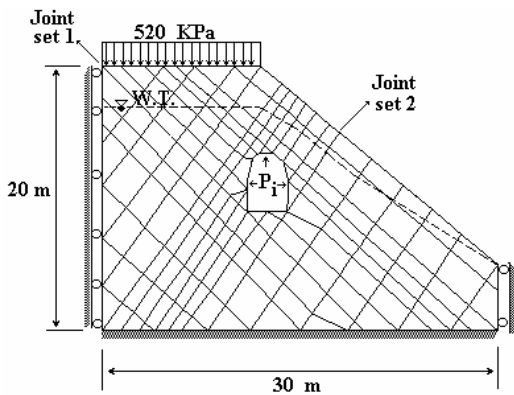


Fig. 21. The geometry and boundary condition

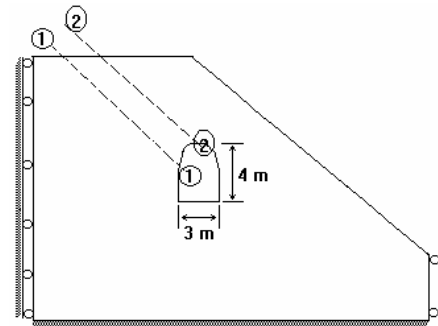


Fig. 22. Arbitrary sections, example 4

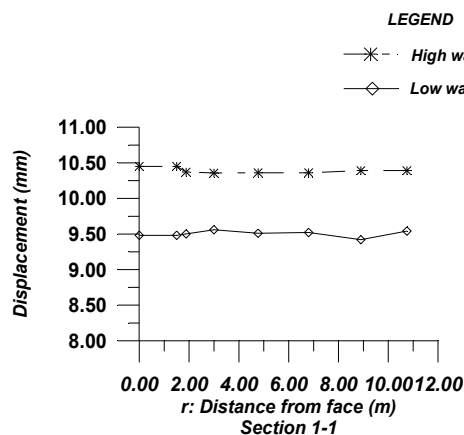


Fig. 23. Comparison of displacements

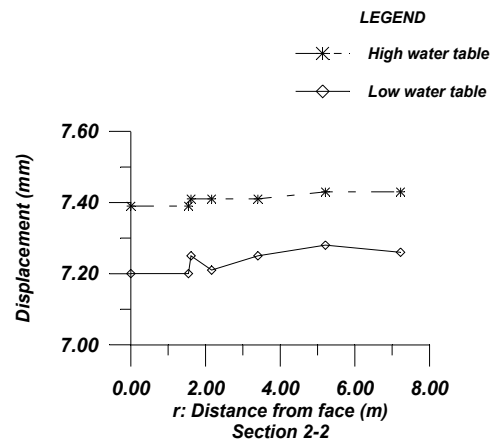


Fig. 24. Comparison of displacements

## 5. CONCLUSIONS

In this paper a computer code developed using a block-spring model was described. A simple method for determination of contact points between blocks was used. The results of analysis using the code were compared with published results to show the adaptability and capability of the program. The effect of incremental loading was also considered and it was shown that load stepping might increase the accuracy of calculations. As it was shown in this paper, although the model in its present format simulates most practical cases of rock mass behavior in a simpler manner compared to other methods, it is these authors intention to strengthen the method and modify it further by introducing damping factor and dynamic equilibrium equations in the near future.

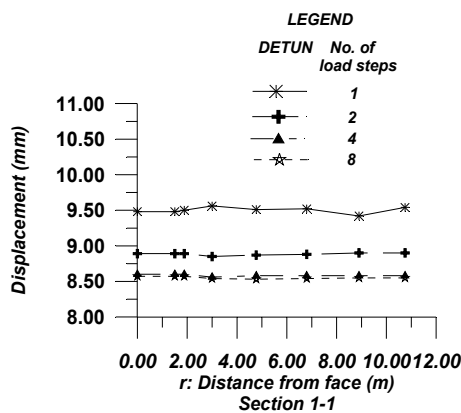


Fig. 25. The effect of incremental loading

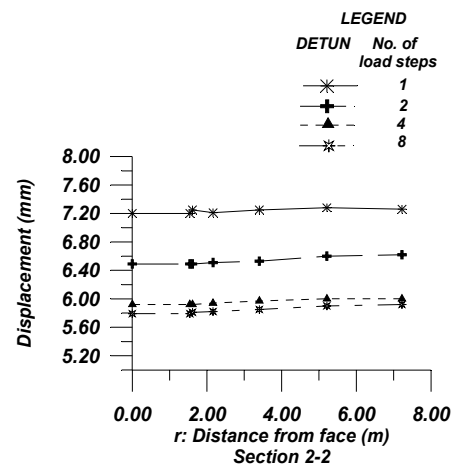


Fig. 26. The effect of incremental loading

## REFERENCES

1. Goodman, R. D., Taylor, R. L. & Brekke, T. L. (1968). A model for the mechanics of jointed rock. *ASCE Journal of the Soil Mechanics and Foundations Division*, 14(SM3), 637-659.
2. Ghaboussi, J., Wilson, E. L. & Isenberg, J. (1973). Finite elements for rock joints and interfaces. *ASCE Journal of the Soil Mechanics and Foundations Division*, 99(SM10), 833-848.
3. Zienkiewicz, O. C., Valliappan, S. & King, I. P. (1968). Stress analysis of rock as a 'no-tension' material." *Geotechnique*, 18, 56-66.
4. Burman, B. C. (1974). Development of a numerical model for discontinua. *Australian Geomechanics Journal*, G4(1), 13-22.
5. Cundall, P. A. (1971). A computer model for simulating progressive large scale movements in blocky rock systems. *Proceedings of the International Symposium on Rock Fracture*, 1(2-8). Nancy, France.
6. Kawai, T. (1977). A new discrete analysis of nonlinear solid mechanics problems involving stability, plasticity and crack. *Proceedings of the Symposium on Applications of Computer Methods in Engineering* (1029-1038). Los Angeles, Calif.
7. Belytschko, T., Plesha, M. & Dowding, C. H. (1984). A computer method for stability analysis of caverns in jointed rock. *International Journal for Numerical and Analytical Methods in Geomechanics*, 8, 473-492.
8. Stewart, I. J. & Brown, E. T. (1984). A static relaxation method for the analysis of excavations in discontinuous rock. Design and performance of underground excavations. *Proceedings of the International Society of Rock Mechanics* (149-155). Edited by E. T. Brown, J. A. Hudson, British Geotechnical Society, London, U.K.
9. Ching, S. C. (1992). Discrete element method for slope stability analysis. *Journal of Geotechnical Engineering*, 118(12), 1889-1905.

10. Wang, B. & Garga, V. K. (1993). A numerical method for large displacements of jointed rocks, I-Fundamentals. *Canadian Geotechnical Journal*, Vol. 30, 96-108.
11. Wang, B. & Garga, V. K. (1993). A numerical method for large displacements of jointed rocks, II-Modeling of rock bolts and groundwater and applications. *Canadian Geotechnical Journal*, 30, 109-123.
12. Hamajima, R., Kawai, T., Yamashita, k. & Kusabuka, M. (1985). Numerical analysis of cracked and jointed rock mass. *Proceedings, 5th International Conference on Numerical Methods in Geomechanics* (207-214). Nagoya, Japan.
13. Tran, T. X. & Nelson, R. B. (1996). Analysis of disjoint two-dimensional particle assemblies. *ASCE Journal of Engineering Mechanics*, 122(12), 1139-1148.
14. Baharloo, M. H. (1998). An investigation on stability of tunnels in rock mass using discrete element method, DEM. M.Sc. Thesis, Shiraz University.